

# Groundwater flow modeling in the Zhangye Basin, Northwestern China

X. H. Wen · Y. Q. Wu · L. J. E. Lee · J. P. Su ·  
J. Wu

Received: 25 September 2006 / Accepted: 12 December 2006 / Published online: 4 January 2007  
© Springer-Verlag 2006

**Abstract** The Zhangye basin is in the middle reaches of the Heihe River, northwestern China. Heavy abstraction of groundwater since the 1970s in the area is for agricultural, industrial and drinking water supplies and has led to a substantial decline in the potentiometric surface. A three-dimensional regional numerical groundwater flow model, calibrated under transient conditions, has been developed and used to predict the drawdown for the period from 2000 to 2030 under two different groundwater management scenarios.

**Keywords** Numerical modeling · Groundwater flow · Groundwater drawdown · Zhangye basin Heihe River · Northwestern China

## Introduction

In the arid northwest of China, water resources play a dominant role in the development of the economy. Careful management is important for ecological and environmental protection (Gao and Li 1990; Cheng and Qu 1992a, b; Feng et al. 2000). The Zhangye basin, in the middle reaches of the Heihe River (Fig. 1), is an important center for development of agriculture and industry (Wang and Gao 2002). For the last few decades, surface water has been the main water supply for the development of agricultural and industrial activities.

Water demands have become greater and groundwater is a secondary source. In the 1970s, the annual exploitation of groundwater was  $0.39 \times 10^8 \text{ m}^3$  and by 1999, this had risen to  $2.17 \times 10^8 \text{ m}^3$ . Due to extensive use of surface water and over abstraction of groundwater, the local springs dried up and water levels were significantly lowered. The quality of groundwater was also impacted (Wang et al. 1999; Tang and Zhang 2001; Ding and Zhang 2002; Liu et al. 2002).

Increasing demand for groundwater will require effective management, and the present study was carried out with that objective by developing a regional groundwater flow model to predict the behavior of groundwater levels in the Zhangye basin over the next 30 years.

## Study site

The Zhangye basin covers an area of  $1.08 \times 10^4 \text{ km}^2$ , extending between latitudes  $38^\circ 30' - 39^\circ 50' \text{N}$  and longitudes  $99^\circ 10' - 100^\circ 52' \text{E}$ , and including Zhangye city, Linze County and Gaotai County (Fig. 1). The area has an arid continental climate with a mean annual temperature of about  $3 - 7^\circ \text{C}$ . The average annual precipitation ranges from 50 to 150 mm. The majority of rain (~80%) falls from June to September. The average potential evaporation rate is about 2,000–2,200 mm/year (Gao 1991).

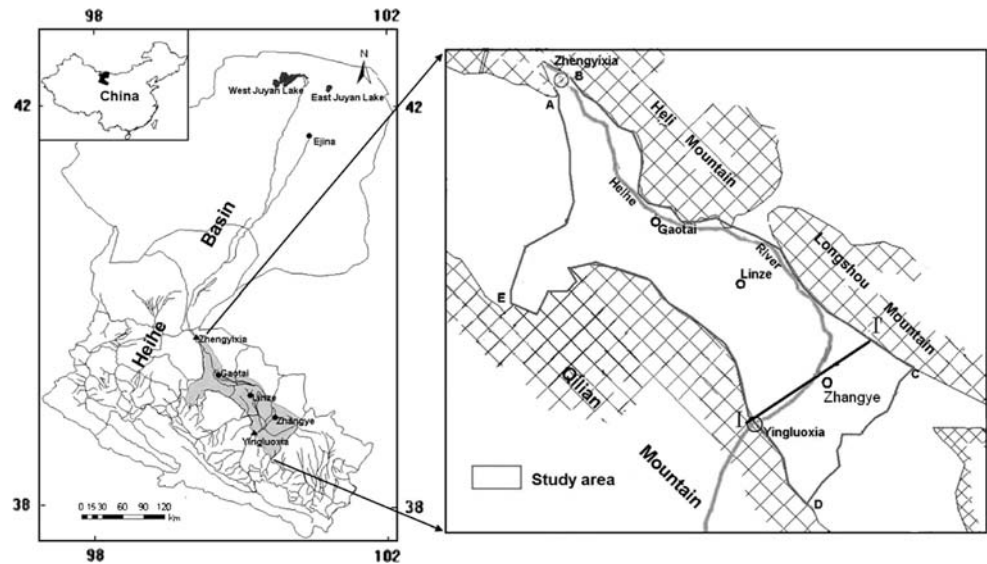
X. H. Wen (✉) · Y. Q. Wu · L. J. E. Lee ·  
J. P. Su · J. Wu

School of Environmental Science and Engineering,  
Shanghai Jiaotong University, Dongchuan Rd 800,  
Shanghai 200240, China  
e-mail: wenxiaohu@gmail.com

## Hydrogeology

The hydrogeological setting was described by Fan (1981) and Chen (1997), which varies from south to

**Fig. 1** Location map of the study area



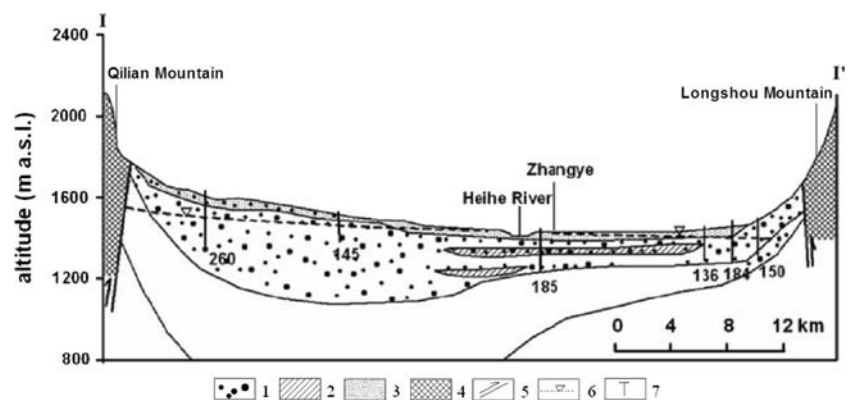
north. The southern part of the basin is an area of extensive faulting, underlain by bedrock. Down-faulted bedrock (pediments) extends toward the northeast, overlain by Quaternary sediments. The uplift of the Qilian Mountains caused the accumulation of several thousand meters of alluvial fan and fluvial deposits in a north-south trending basin. This basin is underlain by Tertiary red molasses, and filled with large volumes of unconsolidated Quaternary sediments, to depths of 300–500 m (Fig. 2). The Quaternary basins can be divided into discrete geomorphologic units, including piedmont alluvial plain, alluvial plain, and desert. The sediments in the basins from south to north gradually change from coarse-grained gravel to medium and fine-grained sand and silt. These sediments along with aeolian and lacustrine deposits form the main aquifers. In the southern part of Zhangye basin, the aquifer is formed from highly permeable cobble and gravel deposits with a thickness of 300 to 500 m. From the northern edge of this diluvial fan, the aquifer becomes confined or semi-confined, with a thickness of

100–200 m, comprising interbedded cobble, gravel, fine sand and clay. Further north, the groundwater table becomes shallow (Fig. 2). A NW-SE thrust fault is present along the foot of the Qilian Mountains. This produces a steep hydraulic gradient. It is difficult for mountain groundwater to flow into the basin by lateral flow and therefore it moves to the surface as springs at the foot of the mountain (Fan 1981; Chen 1997). The rivers originating from the Qilian Mountains are the main source of recharge for the local aquifers. Groundwater in the basin flows generally from the piedmont area towards the centre of the basin. The Longshou and Heli Mountains act as a barrier for groundwater flow, and groundwater discharges at the low part of the basin by upward seepage and springs.

### Conceptual model of the groundwater system

The conceptual model of the hydrogeologic system is based upon the geology from boreholes and water-

**Fig. 2** Hydrogeological cross section along transect I–I' indicated in Fig. 1 (After Chen et al., 2006). 1 gravel, 2 clay, 3 sand, 4 base rock, 5 fault line, 6 groundwater table, 7 borehole and depth



level fluctuation in observation wells. The aquifer is classified into five hydrogeological layers; however, only one layer is present throughout the study area. It is an unconfined aquifer, consisting of gravel intercalated with sandstone layers. In the northern part of the model area, layers two and four consist of sandy clay. In the middle part of the area, they are interbedded with impermeable shale and clay beds or lenses, which cause local or sub-regional confinement of water. Layers three and five consist of medium and fine-grained sand and are confined or semi-confined aquifers. Layers two, three, four and five are only present in the middle part of the basin. The depth of the modeled area varies between 100 and 500 m (Fig. 3).

**Boundary conditions**

Groundwater flow in the aquifer is governed by the boundary conditions of the regional system. Boundary conditions are shown for layer one in Fig. 1. A no-flow boundary was defined between points A–E in the basin, because a groundwater divide is present at this point. Constant head cells were defined between points A–B, because it is coincident with the Zhengyixia reservoir. Along the boundary B–C, the magnitude of groundwater inflow from the mountains to the plain cannot be exactly quantified. A previous study reported that the groundwater inflow is very small and can be neglected (Fan 1981). This boundary was therefore represented as a no-flow boundary. At the boundary D–E, down-faulting occurs and a no-flow boundary condition was applied. Specified flux conditions were defined along the C–D border as shown in Fig. 1. The boundary conditions were only applied to the first layer of the model, while for layers 2–5, the boundary was considered to be impermeable along all model edges.

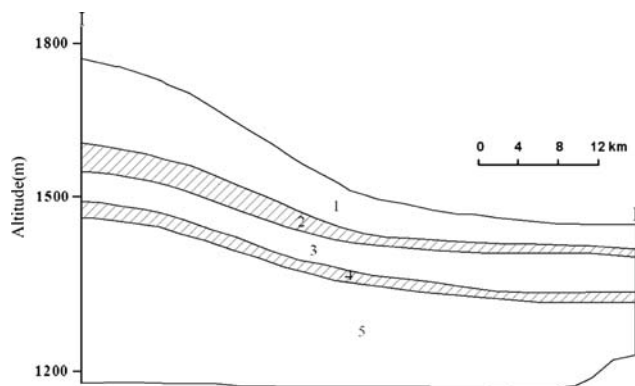


**Fig. 3** Cross section along I–I'

**Initial conditions**

The calibration period was chosen as 1997–2000, because of the availability of relatively complete historical records of hydraulic head at a number of observation wells. To start the calculations, an initial distribution of groundwater head throughout the area was determined. A previous study by Fan (1981) indicated that all the aquifer layers (Fig. 2) were hydraulically connected. Due to the absence of sufficient monitoring wells in all aquifer layers, it was assumed that all aquifers had the same potentiometric surface. An initial spatial distribution of hydraulic head was obtained from 37 observation wells in January of 1997 and a kriging algorithm was used to interpolate these values for the five aquifer layers as shown in Fig. 4.

**Groundwater discharge**

The discharge from the Zhangye basin occurs as springs and through evapotranspiration. The annual volume discharged from the springs is about  $7.93 \times 10^8 \text{ m}^3$  (Li et al. 2004). Groundwater discharge from evapotranspiration is neglected when it is deeper than 4.5 m. The volume of evapotranspiration is about  $3.04 \times 10^8 \text{ m}^3$  per year (Li et al. 2004). The annual volume abstracted for agriculture is about

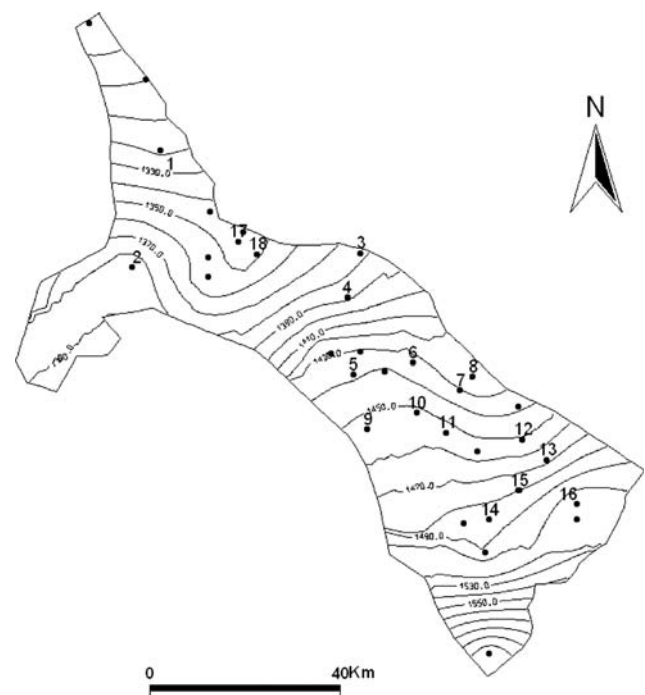


**Fig. 4** Initial values used for groundwater levels in the model (Dots indicate observation wells)

$2.12 \times 10^8 \text{ m}^3$  (Li et al. 2004). The volume abstracted for industrial and domestic activities is about  $0.05 \times 10^8 \text{ m}^3$  per year (Li et al. 2004).

### Groundwater recharge

Recharge to the aquifer varies considerably owing to land-use pattern, soil type, topography and relief. The area was divided into 26 zones based on the irrigation units shown in Fig. 5. Local recharge is inflow from the Heihe River, irrigation return flow and direct recharge. Leakage between Heihe River and the aquifer is the principal source of groundwater recharge. The average direct annual volume of recharge into the aquifer from the Heihe River is about  $5.82 \times 10^8 \text{ m}^3$  (Li et al. 2004). This value was estimated using the difference between river and groundwater levels. Considering the contribution of the canal to recharge in the area, the average direct annual volume of recharge into the aquifer from the canal is about  $3.69 \times 10^8 \text{ m}^3$ .

Irrigation return flow replenishes groundwater based on rock and soil types, and occurs only in the regions where the groundwater depth is shallower than 10 m. The average direct annual volume of recharge into the upper aquifer from irrigation return flow is about  $2.47 \times 10^8 \text{ m}^3$  (Li et al. 2004). For recharge values based on rock and soil types, the average direct annual recharge into the upper aquifer from rainfall is

about  $0.54 \times 10^8 \text{ m}^3$  (Li et al. 2004). The remaining water withdrawn from the aquifer is taken from groundwater storage rather than groundwater recharge. This is estimated as  $0.62 \times 10^8 \text{ m}^3$  annually and has resulted in the steady decrease in groundwater levels in the basin.

### Groundwater flow model

#### Numerical modeling

The anisotropic and heterogeneous three-dimensional flow of groundwater with constant density can be described using the partial differential equation given by Rushton and Redshaw (1979). This equation was used to model groundwater flow in this study. The numerical model for the regional groundwater flow was developed using FEFLOW software (Dierch 1998a, b).

#### Model structure

Spatially, the 3-dimensional model domain is coincident with the study area and covers a surface area of  $5,024.4 \text{ km}^2$ . The domain was discretized into 35,760 triangular prismatic mesh elements with 22,758 nodes in the horizontal orientation. The thickness of the aquifer varied from 200 to 500 m. The finite element grid was generated automatically with moderate refinement along the model boundaries and stream nodes.

#### Model inputs

The model inputs include the hydrogeological parameters hydraulic conductivity ( $K$ ), transmissivity ( $T$ ) and storativity ( $S$ ). The aquifer properties, such as horizontal hydraulic conductivity ( $K_h$ ) and vertical hydraulic conductivity ( $K_v$ ), used in the model were derived from pumping tests. An initial spatial distribution of hydraulic conductivity was obtained from the available data (47 measurements obtained from layers 1 and 2). Data were spatially interpolated using kriging and the corresponding results were divided into arbitrary zones. The hydraulic conductivity in layer 1 was obtained from the available data (35 measurements) and divided into 21 zones of different  $K$  value, ranging from more than 120 m/day in the south of the plain, and decreasing towards the north of the aquifer to less than 1 m/day. The hydraulic conductivity of layer two was obtained from the available data (12 measurements) and divided into 8 zones, with  $K$  values greater

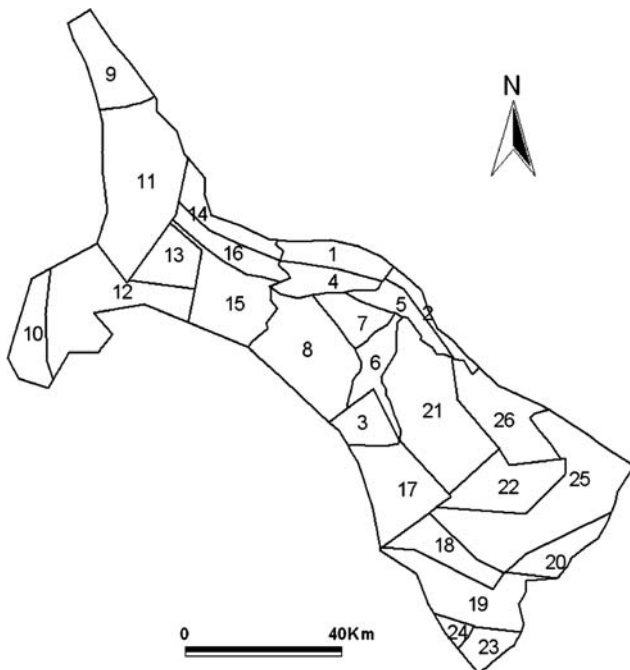


**Fig. 5** Recharge zones

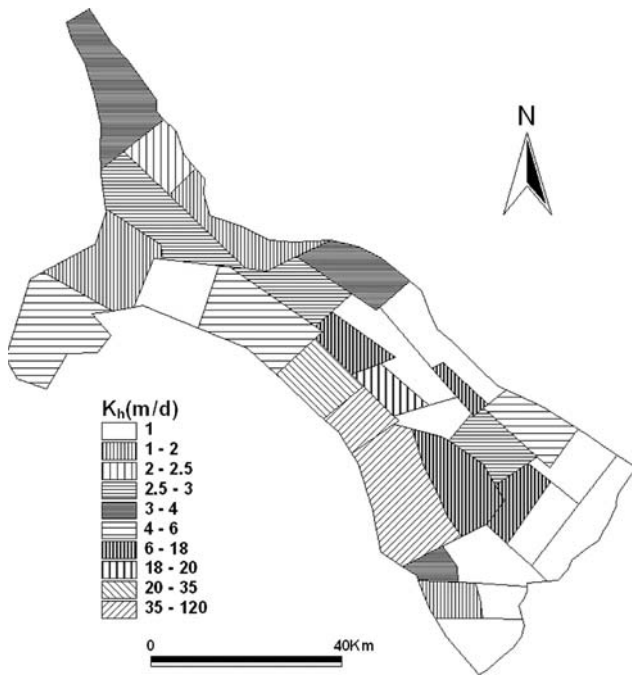


**Fig. 6** Hydraulic conductivity distribution in layer 1

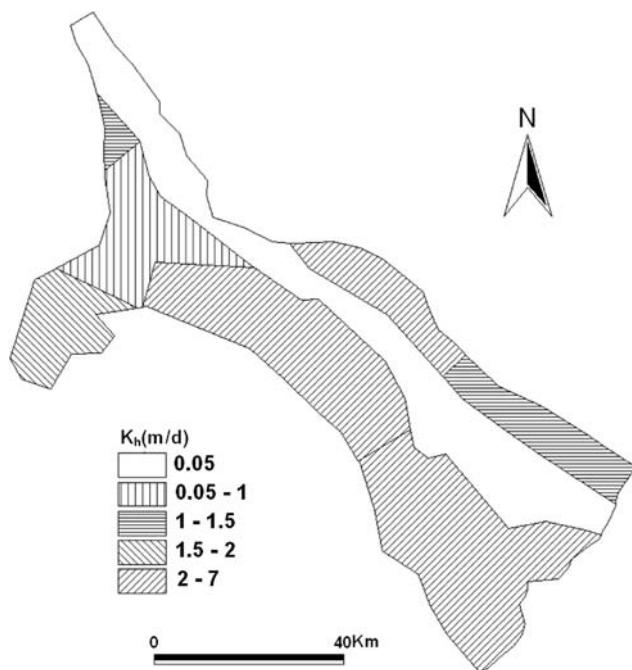


**Fig. 7** Hydraulic conductivity distribution in layers 2 and 4

than 7 m/day in the south of the plain, and decreasing towards the middle and north parts of the aquifer to less than 0.05 m/day. Pumping test data were not available for layers three, four and five. Therefore the hydraulic conductivity data of layer two were applied to layer four, as both layers are sandy clay. The

hydraulic conductivity of layers three and five were based on the data of layers one and two. The hydraulic conductivity of layer three and five were divided into ten zones. In layers three and five hydraulic conductivity is greater than 5 m/day south of the plain, and decreases towards the northern parts of the aquifer to less than 0.15 m/day. As sedimentary rocks are generally much more permeable in the horizontal direction, a vertical anisotropy factor of  $K_h/K_v = 10$  was assumed for all layers (Freeze and Cherry 1979). Specific yield ( $S$ ) and specific storage were also assigned to the model. The values of specific yield ranged from 0.01–0.28 and were obtained from pumping tests; a value of  $10^{-5}$  was assigned to specific storage.

**Model calibration**

Before the model was used to forecast future groundwater levels, calibration was carried out using historical groundwater-level data. A transient simulation was undertaken for the four-year period from January 1997 to December 2000 with a monthly time step. The hydraulic conductivity values incorporated in the transient model were modified during calibration, obtaining 31 final zones of hydraulic conductivity in layer 1 (Fig. 6). This final zonation was in agreement with the observed ranges of the hydraulic conductivities and followed the spatial trend of the initially interpolated values (Figs. 6, 7, 8). The spatial distribution of specific yield was also modified during calibration. The transient models were calibrated satisfactorily (Fig. 9), based on the close agreement between computed and observed heads from January 1997 to December 2000 at 18 observation wells (Fig. 4) distributed throughout the aquifer.

The sensitivity of the model to input parameters was tested by varying only the parameters of interest over a range of values, and monitoring the response of the model by determining the root mean square error of the simulated heads compared to the measured heads. These analyses showed that the model is most sensitive to recharge.

Contour maps (Fig. 10) of simulated groundwater levels versus observed groundwater levels indicate fairly good agreement. Time series of computed and observed heads in wells 1, 4, 9 and 15 are shown in Figure 11. Well 1 is north of the basin in a highly irrigated area near Heihe River. Infiltration of irrigation water causes a rise over time in the local groundwater table. In the southern part of the basin, the abstraction of surface water has increased and recharge of groundwater has decreased. The groundwater table has therefore gradually declined (wells

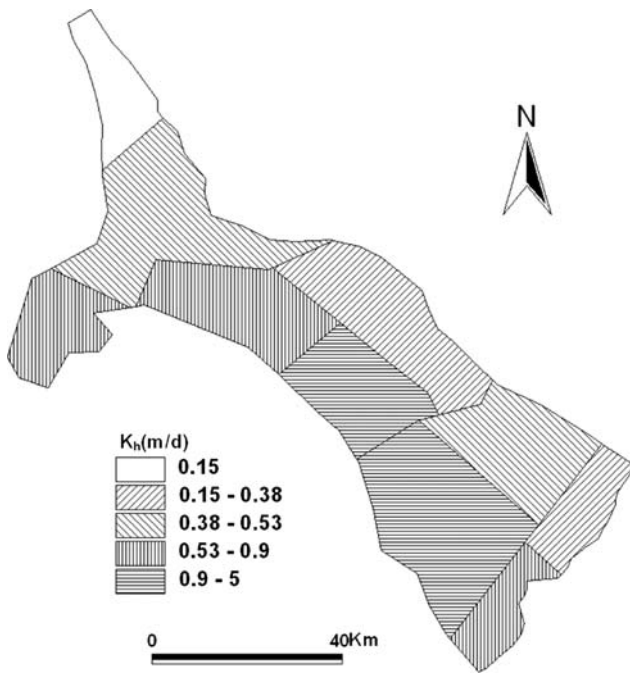


**Fig. 8** Hydraulic conductivity distribution in layers 3 and 5

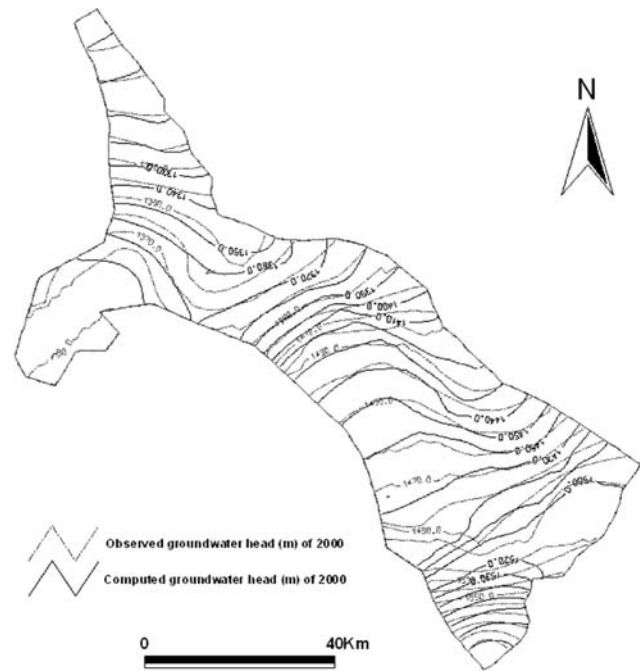


**Fig. 10** Comparison of computed and observed groundwater levels in 2000

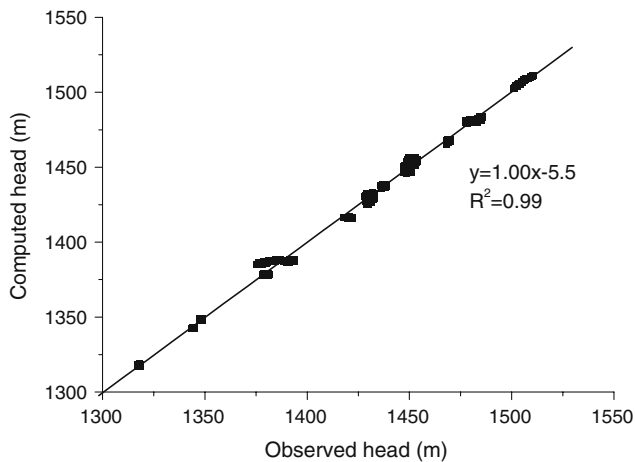


**Fig. 9** Computed versus simulated groundwater head under transient-state calibration

9 and 15) over four years. In the middle part of the basin (well 4), the groundwater levels have remained approximately constant.

#### Assessment and evaluation of planned groundwater development

The calibrated model was used to evaluate two plans for potential exploitation of groundwater in the

Zhangye basin, with the objective of predicting aquifer drawdown. Simulations were made for the period 2000–2030. Scenario 1 assumed that the present exploitation rates were steady for the period 2000–2030. Scenario 2 entailed a reduction in groundwater abstraction year by year for irrigation over the entire basin. The annual volume of groundwater abstraction was assumed to be  $1.4 \times 10^8 \text{ m}^3$  by the year 2030 (Li et al. 2004), with a decrease each year of  $0.025 \times 10^8 \text{ m}^3$  from the current annual value of  $2.17 \times 10^8 \text{ m}^3$ . Figures 12 and 13 show the contours of drawdown for scenarios 1 and 2 for the end of the simulation period, i.e., 2030. The pattern of drawdown is similar for both scenarios, with a drawdown of less than 10 m present far northwest of the basin and along the northeastern edge, following the course of Heihe River. In scenario 1, the maximum drawdown in the south is 30 m by 2030. For scenario 2, a large groundwater drawdown also occurs by 2030 (Fig. 13). In scenario 2 the value and range of the hydraulic head drawdown is less than scenario 1, reaching a maximum of 24 m in the south. In the middle part of the basin, the groundwater head is stable under the scenario 2 pumping rate. This suggests that reduction of the abstraction rate may reduce the drawdown of overall hydraulic head in some areas of the basin.

**Fig. 11** Simulated and observed head at observation wells 1, 4, 9 and 15

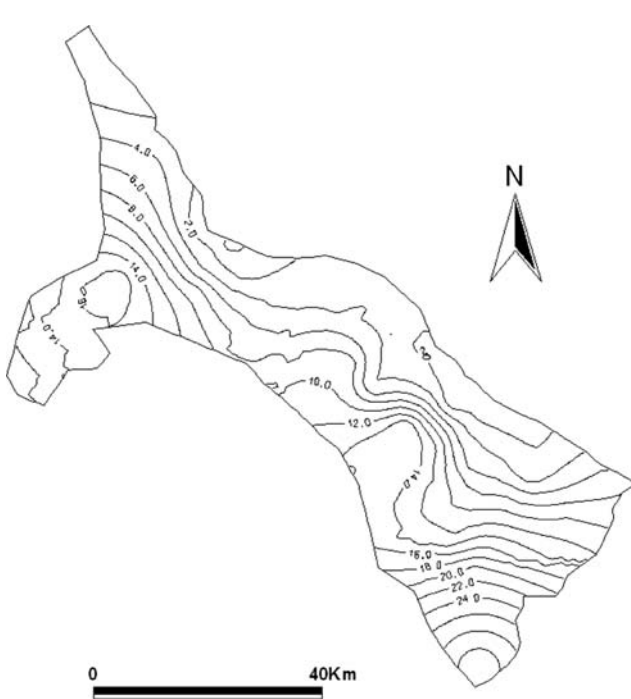
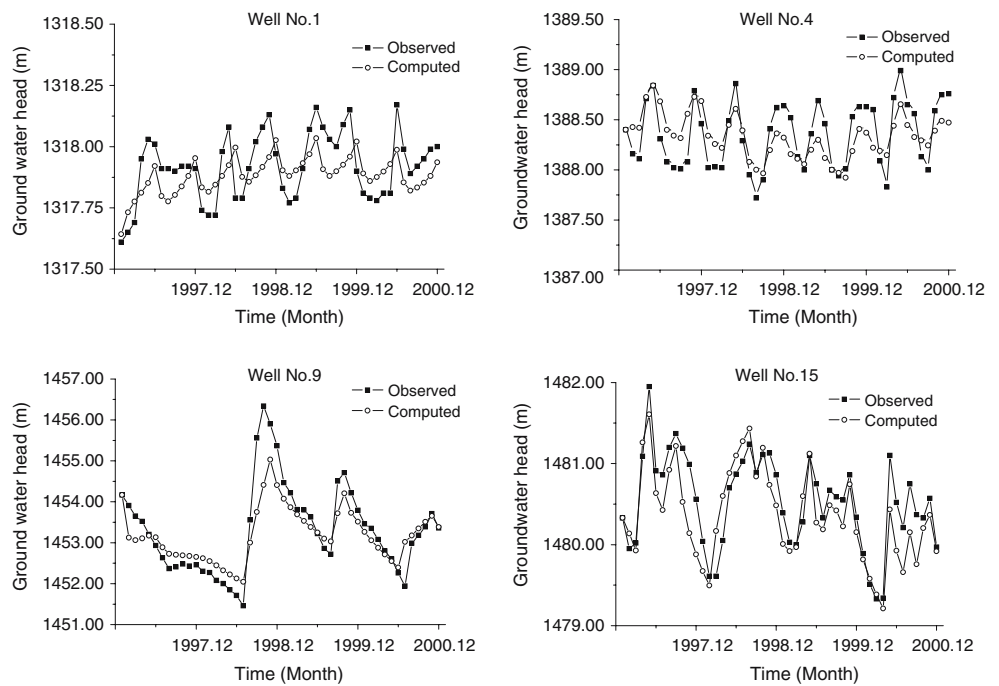


**Fig. 12** Contours of groundwater drawdown for 2030, scenario 1

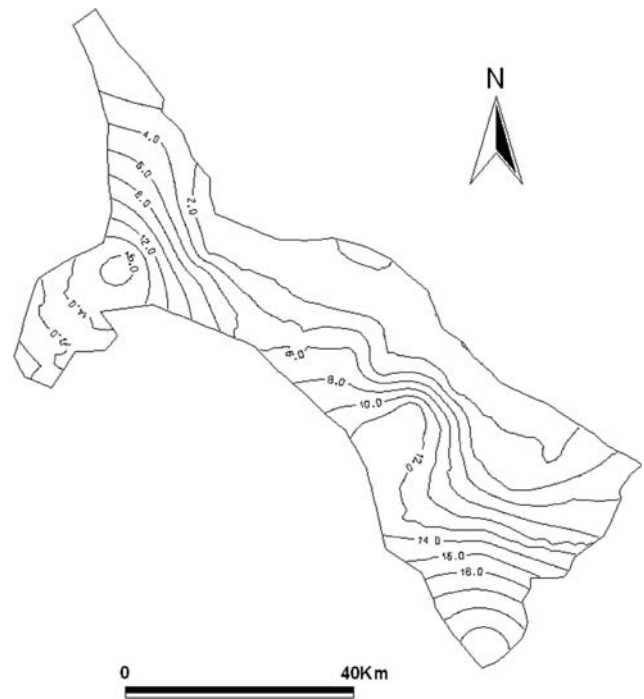


**Fig. 13** Contours of groundwater drawdown for 2030, scenario 2

**Conclusion**

The sedimentary aquifers of the Zhangye basin were investigated using FEFLOW to simulate three-dimensional groundwater flow under transient conditions. The results of the model calibration show reasonable

agreement between observed and calculated water levels for the observation wells.

The calibrated model was used to predict the drawdown for the period from 2000 to 2030 under two different abstraction scenarios. In scenario 1, the groundwater abstraction remains steady until 2030; in

scenario 2, the groundwater abstraction is reduced over the same period. Under scenario 1, the predicted maximum drawdown south of the basin in 2030 is 30 m. Under scenario 2 the value and range of the hydraulic head drawdown is less than in scenario 1, reaching a maximum of 24 m south of the basin in 2030. In the middle part of the basin, the aquifer system is stable under the scenario 2 pumping rate. This suggests that reduction of the abstraction rate may reduce the drawdown of overall hydraulic head in some areas of the basin.

**Acknowledgments** This work was supported by the Postdoctor Science Foundation of China (20060390632), National Science Foundation of China (10572090). The authors wish to thank the anonymous reviewers for their reading of the manuscript, and for their suggestions and critical comments.

## References

- Anderson MP, Woessner WW (1992) Applied ground water modeling: simulation of flow and advective transport. Academic, New York
- Chen MX (1997) The water resources related with Quaternary basin system in arid area of Northwest China. *Q Sci Rev* 16:97–104
- Chen ZY, Nie ZL, Zhang GH, Wan L, Shen JM (2006) Environmental isotopic study on the recharge and residence time of groundwater in the Heihe River Basin, northwestern China *Hydrogeol J*. doi:10.1007/s10040-006-0075-7
- Cheng L, Qu Y (1992a) Water and land resources and their rational development and utilization in Heixi region. Beijing: Science Press, pp 36–169 (in Chinese)
- Cheng L, Qu Y (1992b) Water and land resources and their rational development and utilization in the Hexi region. Science Press, Beijing (in Chinese)
- Dierch H-JG (1998a) FEFLOW—reference manual. WASI—Institute of Water Resources Planning and System Research Ltd., Berlin
- Dierch H-JG (1998b) FEFLOW—users manual. WASI—Institute of Water Resources Planning and System Research Ltd., Berlin
- Ding H, Zhang J (2002) The problem of environmental caused by groundwater level continuous decline in the inland basins of arid area, Northwest China – an example in middle reaches of Heihe river basin. *Hydrogeology and Engineering Geology* 3:71–75 (in Chinese)
- Feng Q, Cheng G, Masao MK (2000) Trends of water resources development and utilization in arid north-west China. *Environ Geol* 39(8):831–838
- Freeze RA, Cherry JA (1979) Ground water. Prentice-Hall, Inc., Englewood Cliffs
- Fan X (1981) Transformation of groundwater and surface water and rational utilization of water resources in Hexi Corridor region (in Chinese). *Hydrogeol Eng Geol* 4:1–6
- Gao Q, Li F (1990) Rational development and utilization of water resources in Heihe basin (in Chinese). Gansu Press of Science and Technology, Lanzhou, pp 23–95
- Gao Q (1991) Development and utilization of water resources in the Heihe River catchment (in Chinese). Gansu Science and Technology Press, Lanzhou, p 205
- Liu S, Lu Y, Cheng X, Yang Z (2002) Groundwater system and water resources environmental effect induced water resources development in the middle and lower reaches of Heihe River. *Geogr Territorial Res* 18(4):90–96
- Li Z, Zhao C, Yang J (2004) The study of water resources system and macroscopic adjustment and control in the inland river basin, northwestern China (in Chinese). Lanzhou, China pp 44–64
- Rushton KR, Redshaw SC (1979) Seepage and groundwater flow. Wiley, New York
- Tang Q, Zhang J (2001) Water resources and eco-environment protection in the arid regions in northwest of China (in Chinese). *Progr Geogr* 20(3):227–233
- Wang X, Gao Q (2002) Sustainable development and management of water resources in the Hei River Basin of Northwest China. *Water Resources Development* 18(2):335–352
- Wang G, Cheng G, Yang Z (1999) The utilization of water resources and its influence on eco-environment in the northwest arid area of China (in Chinese). *J Nat Resources* 14(2):109–116